[Brief Communication]

Structural and functional glycosphingolipidomics by glycoblotting with aminooxy-functionalized gold nanoparticle

Noriko Nagahori[1], Midori Abe[1], and Shin-Ichiro Nishimura[1,2]*

[1]*Laboratory for Advanced Chemical Biology, Graduate School of Advanced Life Science, and Frontier Research Center for the Post-Genome Science and Technology, Hokkaido University, N21, W11, Sapporo 001-0021, Japan*

[2]*Drug-Seeds Discovery Research Laboratory, National Institute of Advanced Industrial Science and Technology (AIST), Sapporo 062-8517, Japan*

*To whom correspondence should be addressed.

E-mail: shin@glyco.sci.hokudai.ac.jp

The first paragraph (144 words).

Glycosphingolipids (GSLs) synthesized in Golgi apparatus by sequential transfer of sugar residues to a ceramide lipid anchor are ubiquitously distributing on vertebrate plasma membranes. Standardized method allowing for high throughput structural profiling and functional characterization of living cell surface GSLs is of growing importance because they function as crucial signal transduction molecules in various processes of dynamic cellular recognitions. However, methods are not available for amplification of GSLs, while the genomic scale PCR amplification permits large-scale mammalian genomics and proteomics. Here we communicate such an approach to a novel *"omics"*, namely glycosphingolipidomics based on the *glycoblotting* method. The method, which involves selective ozonolysis of the C-C double bond in ceramide moiety and subsequent enrichment of generated GSL-aldehydes by chemical ligation using aminooxy-functionalized gold nanoparticle (aoGNP) should be of widespread utility for structural identification and functional characterization of whole GSLs present in the living cells/tissues.

Main text (1424 words).

Cell surface GSLs exhibit various and crucial functions in cell growth, differentiation, adhesion, and malignant alteration[1]. It has been documented that dramatic changes in GSL composition and metabolism are strongly associated with oncogenic transformation[2,3]. Therefore, identification of disease-related structural alteration of cell surface GSLs will become a key to develop diagnostic biomarkers and therapeutic anticancer vaccines. However, purification and structural characterization of cellular GSLs have not been routinely possible to date, typically requiring tedious and time-consuming extraction/purification steps of GSLs of interest from extremely complex mixtures before analysis. In general, protocols for the isolation of GSLs would vary depending upon the analytical methods as well as chemical properties of individual GSLs and would need specialized expertise at step-by-step/case-by-case handling for separation. These crucial problems in the enrichment of whole GSLs make it difficult to achieve high throughput structural and functional analyses of biologically important GSLs. In addition, we should pay attention to the fact that cell surface GSLs often exhibit specific biological functions through dynamic mechanism such as clustering or

self-assembling in order to amplify the affinity with partner molecules. For example, it was suggested that tumor-associated GSLs are locating at high density in tumor cells and may be organized in microdomains at the tumor cell surface[4,5]. It seems that self-assembly of GSLs might become an essential mechanism to serve their immunogenicity and antigenicity[1]. We thought that a practical method allowing both for structural profiling and for functional analysis of GSLs as key component of cell surface microdomain is now strongly expected.

We have demonstrated the versatility of chemical ligation of reactive carbonyl groups by means of aminooxy- or hydrazine-functionalized polymers in selective enrichment analysis of whole *N*-glycans[6-12] and some kinds of glycopeptides[8,13] derived from human serum, cellular glycoproteins, and biopharmaceuticals. The new concept of "*glycoblotting*", a glycan enrichment technology based on the above chemical ligation, greatly facilitated further quantitative and large-scale glycomics and glycoproteomics using general mass spectrometry-based analyses for the purpose of exploring clinically potential biomarkers[11-13].

On the other hand, it is well known that metal and semi-conducting nanoparticles

are nice tools of the scaffold materials displaying various biomolecules through the specific Au-S bonding[14]. Since these nanoparticles conjugated with biomolecules are soluble or well dispersed in aqueous solution and stable under physiological conditions, they have been widely applied in broad scientific fields of biochemistry and chemical biology for the molecular recognition assay[15,16]. Metal nanoparticles have also been used as a matrix for LDI-MS analysis, where the metal particles serve as a reservoir for photon energy deposition[17,18]. Advantages of the use of gold nanoparticle (GNP) in MALDI-TOFMS based structural characterization may be summarized as follows: (a) GNP exhibits much greater ionization efficiency than common organic matrices due to the quantum coefficient effect[19], (b) self assembled monolayer (SAM) of thiol compound chemisorbed onto the Au surface can be ionized efficiently to cleave the Au-S bond by laser irradiation in the MALDI process[20], and (c) conjugating mass-limited small molecules onto the colloidal Au surface makes it possible to sequester and transfer small quantities of analytes with high efficiency[21]. Recent our results revealed that ionization of analytes is highly enhanced by specific laser-scattering or diffused reflection on the extremely increased surface area of metal

nanoparticles, which may greatly accelerate the ionization of chemisorbed small molecules from GNP[22,23]. We hypothesized that a streamlined protocol by integrating above two technologies, "*glycoblotting and GNP-assisted MALDI-TOFMS*", makes an enrichment analysis of living cell surface glycosphingolipids possible. Here we communicate for the first time a comprehensive approach of structural and functional glycosphingolipidomics based on glycoblotting method.

Naturally occurring GSLs commonly involve a *trans*-double bond at C-4,5 position of the sphingosine base moiety, which can be cleaved quantitatively by simple ozonolysis to generate aldehyde derivatives of the parent GSLs (**Figure 1**). This characteristic feature of GSLs prompted us to establish novel and standardized method allowing for structural and functional glycosphingolipidomics concurrently. **Figure 2(a)** illustrates a general strategy for the selective enrichment of cellular GSLs onto GNP surface by applying the concept of glycoblotting. We devised high performance and well dispersed GNP having aminooxy functional groups (aoGNP) by reduction of Au^{3+} ion ($KAuCl_4$) with $NaBH_4$ in the mixed solution of methanol and water in the presence of stabilizing reagents 11,11'-dithio bis[(undec-11-yl)-

12-(*N*-{*tert*-butoxycarbonyl}aminooxyacetyl)amino hexa(ethyleneglycol)] (**1**) and 1,1'-dithio bis[undec-11-yl hexa(ethylene glycol)] (**2**). The average diameter of aoGNP was estimated to be 1.3 nm, indicating that an aoGNP is composed of 79 Au atoms and covered with 38 thiol molecules (The synthesis of compounds **1**, **2**, and MS-based characterization of aoGNP are described in the **Supplementary Information**). It was revealed that the oxime bonds formed between GSL-aldehydes and aminooxy groups of aoGNP can be readily cleaved by laser irradiation under common MALDI condition to afford highly sensitive iminoalcohol ions [**Figure 2(b)**]. To illustrate the new method, crude lipids fraction[24] of C57BL/6JJcl adult (7 weeks) and embryonic (13.5 days) mouse brains were subjected directly to "ozonolysis" and "glycoblotting" protocol. Reaction of GSL-aldehydes with aoGNPs proceeded smoothly under mild condition without any special reagent. After simple purification GSLs transferred onto aoGNPs (GSLs-GNPs) were employed directly for further structural characterization. The merit of this method is evident because whole procedure from GSLs enrichment to mass spectrometry-based structural profiling can be performed within 3~4 hours by employing approximately 100 mg (wet weight) of

mouse brain. As anticipated, MALDI-TOFMS showed that aoGNP captures four major gangliosides such as GM1 (*m/z* 1411.5), GD1a/GD1b (*m/z* 1702.6), and GT1b (*m/z* 1993.6) found in general adult mouse brain and GD3 (*m/z* 1272.6) found mainly in embryonic mouse brain [**Figure 3(a)-(c)**][25]. When GSLs enriched similarly on aoGNP from mouse B16 melanoma cells (1.7×10^7 cells) were subjected to MALDI-TOFMS, multiple ion peaks corresponding to GM3 analogs having various long acyl chains were detected at *m/z* 1037.9 (h18:0), 1065.9 (21:0 or h20:0), 1081.9 (h21:0), 1093.4 (23:0 or h22:0), 1110.0 (h23:0), 1124.1 (h24:0), and 1140.1 (2h24:0) [**Figure 4(a)**]. This result clearly indicates that the present protocol greatly facilitated analysis of the molecular diversity (microheterogeneity) of GSLs in terms of alterations in *N*-acyl groups as well as glycoforms [**Figure 4(b)**].

Next, our interest was focused on the feasibility of aoGNPs as a platform for the characterization of carbohydrate-carbohydrate interaction conducted by cell surface glycosphingolipids[26]. It seems that whole GSLs enriched on the GNPs might become a plausible model of the living cell “microdomain” involving high-density GSLs and serves as nice tools for investigating specific functions of self-assembled GSLs under a

similar topology to the intact plasma membrane. Here we examined the feasibility of aoGNPs for functional analysis of above mentioned B16 cell surface GSLs because it was documented that GM3 is identified as the melanoma-associated antigen in mice, hamsters and humans[27] and microdomain composed of highly expressed GM3 in mouse melanoma B16 cells[28] intermediates cancer metastasis through the specific adhesion with Gg3Cer[29,30]. In addition to GSLs(B16)-GNPs [whole GSLs on aoGNP enriched from mouse B16 melanoma cells described in the above MS analyses (**Figure 4**)], we prepared GSLs-GNPs displaying pure GalCer, LacCer, GM1, and GM3 as controls. The calibration curves were also made by using these authentic GSLs-GNPs to determine the amount of total GSLs enriched from B16 cells on the GNPs. The concentration of GSLs-GNPs was estimated by means of pulsed amperometric analysis using high-pH anion-exchange column chromatography (HPAE-PAD, **Supplementary Methods**). The results indicated that approximately 7~16 molecules of GSLs are captured on the surface of the single aoGNP, respectively (the average surface area of the single GNP = 5.3 nm^2). Thus, well-characterized GSLs-GNPs were employed for further binding assay using surface plasmon resonance (SPR) with LB-membrane of

gangliotriaosylceramide (Gg3Cer) immobilized on gold substrate. It was revealed that the binding profile of GSLs(B16)-GNPs seems to be quite similar to that of GM3-GNPs and the affinity constants (K_a) were calculated by applying above equation to be 4.35×10^5 M^{-1} for GSLs(B16)-GNPs and 3.64×10^5 M^{-1} for GM3-GNPs, respectively (**Figure 5**). On the other hand, the binding curves of other GSLs-GNPs such as GalCer-GNPs, LacCer-GNPs, and GM1-GNPs did not fit to above Langmuir-type isothermal adsorption equation, indicating that they are non-specific binding. These results clearly suggest that the binding of GM3-GNPs or GSLs(B16)-GNPs with Gg3Cer monolayer is a specific and high affinity interaction[30].

In conclusion, we demonstrated that aoGNPs are suited scaffold material for the chemical enrichment (glycoblotting) and subsequent MALDI-TOFMS-based structural characterization of naturally occurring GSLs. Conceptually, this is the first approach to permit high throughput structural profiling of living cell/tissue GSLs. This new protocol, in combination with nanoparticles-based molecular imaging/sensing technology, should help to expedite a novel class glycosphingolipidomics and discovery research of disease-related biomarkers.

METHODS (114 words).

Ozonolysis and enrichment of mouse brain GSLs. Crude lipids fraction of C57BL/6JJcl adult (7 weeks) and embryonic (13.5 days) mouse brain extracted by using Ladisch solvent[24] [diisopropyl ether/1-butanol/50 mM NaCl aq. (6/4/5, v/v/v)] was subjected directly to the treatment with O_3 for 30 min and quenched with triphenylphosphine. The solution containing GSL-aldehydes was washed with diisopropyl ether/1-butanol (3/2, v/v) to remove simple alkyl aldehyde as by-product. Then, the mixture was allowed to react with aoGNPs in 50 mM sodium acetate buffer (pH 4.0 at ambient temperature). After evaporating to complete oxime-bond formation, GSLs-GNPs were collected, washed thoroughly by using simple ultrafiltration, and employed directly for MALDI-TOFMS. For the full protocols see the Supplementary Information.

Acknowledgments

This work is supported by a program grant "Innovation COE program for future drug

discovery and medical care" from JST-Japan. We thank Dr. S. -I. Hakomori, Dr. Y. Igarashi, and Dr. Dr. Y. Nagai for stimulating discussions.

Competing interests statement

The authors declare that they have no competing financial interests.

References

1. Hakomori, S. -I. , Zhang, Y. Glycosphingolipid antigens and cancer therapy. *Chem. Biol.* **4**, 97-104 (1997).

2. Hakomori, S. -I. Tumor malignancy defined by aberrant glycosylation and sphingo(glyco)lipid metabolism. *Cancer Res.* **56**, 5309-5318 (1996).

3. Hakomori, S. -I., Murakami, W. T. Glycolipids of hamster fibroblasts and derived malignant-transformed cell lines. *Proc. Natl. Acad. Sci. USA* **59**, 254-261 (1968).

4. Brown, D. A., London, E. Structure and function of sphingolipid- and cholesterol-rich membrane rafts. *J. Biol. Chem.* **275**, 17221-17224 (2000).

5. Hakomori, S. -I. Bifunctional role of glycosphingolipids. Modulators for

transmembrane signaling and mediators for cellular interactions. *J. Biol. Chem.* **265**, 18713-18716 (1990).

6. Nishimura, S. -I., Niikura, K., Kurogochi, M., Matsushita, T., Fumoto, M., Hinou, H., Kamitani, R., Nakagawa, H., Deguchi, K., Miura, N., Monde, K., Kondo, H. High-throughput protein glycomics: combined use of chemoselective glycoblotting and MALDI-TOF/TOF mass spectrometry. *Angew. Chem., Int. Ed. Engl.* **44**, 91-96 (2005).
7. Niikura, K., Kamitani, R., Kurogochi, M., Uematsu, R., Shinohara, Y., Nakagawa, H., Deguchi, K., Monde, K., Kondo, H., Nishimura, S. -I. Versatile glycoblotting nanoparticles for high-throughput protein glycomics. *Chem. Eur. J.* **11**, 3825-3834 (2005).
8. Shimaoka, H., Kuramoto, H., Furukawa, J., Miura, Y., Kurogochi, M., Kita, Y., Hinou, H., Shinohara, Y., Nishimura, S. -I. One-pot solid-phase glycoblotting and probing by transoximization for high-throughput glycomics and glycoproteomics. *Chem. Eur. J.* **13**, 1664-1673 (2007).
9. Miura, Y., Shinohara, Y., Furukawa, J., Nagahori, N., Nishimura, S. -I. Rapid and

simple solid-phase esterification of sialic acid residues for quantitative glycomics by mass spectrometry. *Chem. Eur. J.* **13**, 4797-4804 (2007).

10. Kita, Y., Miura, Y., Furukawa, J., Nakano, M., Shinohara, Y., Ohno, M., Takimoto, A., Nishimura, S. -I. Quantitative glycomics of human whole serum glycoproteins based on the standardized protocol for liberating *N*-glycans. *Mol. Cell. Proteomics* **6**, 1437-1445 (2007).
11. Furukawa, J., Shinohara, Y., Kuramoto, H., Miura, Y., Shimaoka, H., Kurogochi, M., Nakano, M., Nishimura, S. -I. A comprehensive approach to structural and functional glycomics based on chemoselective glycoblotting and sequential tag conversion, *Anal. Chem.* **80**, 1094-1101 (2008).
12. Miura, Y., Hato, M., Shinohara, Y., Kuramoto, H., Furukawa, J., Kurogochi, M., Shimaoka, H., Tada, M., Nakanishi, K., Ozaki, M., Todo, S., Nishimura, S. -I. BlotGlycoABC^{TM}: An integrated glycoblotting technique for rapid and large-scale clinical glycomics, *Mol. Cell. Proteomics* **7**, 370-377 (2008).
13. Kurogochi, M., Amano, M., Fumoto, M., Takemoto, A., Kondo, H., Nishimura, S. -I. Reverse glycoblotting allows rapid-enrichment glycoproteomics of

biopharmaceuticals and disease-related biomarkers, *Angew. Chem. Int. Engl. Ed*. **46**, 8808-8813 (2007).

14. Katz, E., Willner, I. Integrated nanoparticle-biomolecules hybrid systems: synthesis, properties, and applications. *Angew. Chem. Int. Engl. Ed*. **43**, 6042-6108 (2004).
15. de la Fuente, J. M., Barrientos, A. G., Rojas, T. C., Rojo, J., Canada, J., Fernandez, A., Penades, S. Gold nanoparticles as water-soluble polyvalent models to study carbohydrate interactions. *Angew. Chem. Int. Engl. Ed*. **40**, 2257-2261 (2001).
16. Bruchez, M., Moronne, M., Gin, P., Weiss, S., Alivisatos, A. P. Semiconductor nanocrystals as fluorescent biological labels. *Science* **281**, 2013-2016 (1998).
17. Tanaka, K., Waki, H., Ido, H., Akita, S., Yoshida, T. Protein and polymer analyses up to m/z 100,000 by laser ionization time-of flight mass spectrometry. *Rapid. Commun. Mass. Spectrom.* **2**, 151-153 (1988).
18. Teng, C. H., Ho, K. C., Lin, Y. S., Chen, Y. C. Gold nanoparticles as selective and concentrating probes for samples in MALDI MS analysis. *Anal. Chem.* **76**, 4337-4342 (2004).
19. McLean, J. A., Stumpo, K. A., Russell, D. H. Size-selected (2-10 nm) gold

nanoparticles for matrix assisted laser desorption ionization of peptides. *J. Am. Chem. Soc.* **127**, 5304-5305 (2005).

20. Mouradian, S., Nelson, C. M., Smith, L. M. A self-assembled matrix monolayer for UV-MALDI mass spectrometry. *J. Am. Chem. Soc.* **118**, 8639-8645 (1996).

21. Kirk, J. S., Bohn, P. W. Surface adsorption and transfer of organomercaptans to colloidal gold and direct identification by matrix assisted laser desorption/ionization mass spectrometry. *J. Am. Chem. Soc.* **126**, 5920-5926 (2004).

22. Nagahori, N., Nishimura, S. -I. Direct and efficient monitoring of glycosyltransferase reactions on gold colloidal nanoparticles by using mass spectrometry. *Chem. Eur. J.* **12**, 6478-6485 (2006).

23. Su C. -L., Tseng, W. -L. Gold nanoparticles as assisted matrix for determining neutral small carbohydrates through laser desorption/ionization time-of-flight mass spectrometry. *Anal. Chem*. **79**, 1626-1633 (2007).

24. Ladisch S., Gillard, B. A solvent partition method for microscale ganglioside purification. *Anal. Biochem.* **146**, 220-231 (1985).

25. Ngamukote, S., Yanagishita, M., Ariga, T., Ando, S., Yu, R. K. Developmental

changes of glycosphingolipids and expression of glycogens in mouse brains, *J. Neurochem.* **102**, 2327-2341 (2007).

26. Kojima, N., Hakomori, S. -I. Specific interaction between gangliotriaosylceramide (Gg3) and sialosyllactosylceramide (GM3) as a basis for specific cellular recognition between lymphoma and melanoma cells. *J. Biol. Chem.* **264**, 20159-20162 (1989).

27. Nores, G. A., Dohi, T., Taniguchi, M., Hakomori, S. -I. Density-dependent recognition of cell surface GM3 by a certain anti-melanoma antibody, and GM3 lactone as a possible immunogen: requirements for tumor-associated antigen and immunogen. *J. Immunol*. **139**, 3171-3176 (1987).

28. Hirabayashi, Y., Hamaoka, A., Matsumoto, M., Matsubara, T., Tagawa, M., Wakabayashi, S., Taniguchi, M. Syngeneic monoclonal antibody against melanoma antigen with interspecies cross-reactivity recognizes GM3, a prominent ganglioside of B16 melanoma. *J. Biol. Chem*. **260**, 13328-13333 (1985).

29. Otsuji, E., Park, Y. S., Tashiro, K., Kojima, N., Toyokuni, T., Hakomori, S. -I. Inhibition of B16 melanoma metastasis by administration of G(M3)- or Gg3-

liposomes: Blocking adhesion of melanoma cells to endothelial cells (anti-adhesion therapy) via inhibition of G(M3)-Gg3Cer or G(M3)LacCer interaction. *Int. J. Oncol.* **6**, 319-327 (1995).

30. Iwabuchi, K., Yamamura, S., Prinetti, A., Handa, K., Hakomori, S. -I. GM3-enriched microdomain involved in cell adhesion and signal transduction through carbohydrate-carbohydrate interaction in mouse melanoma B16 cells. *J. Biol. Chem.* **273**, 9130-9138 (1988).

Figure and Scheme Legend

Figure 1. Chemical structures of major glycosphingolipids used in this study.

Figure 2. (a) A general strategy for structural and functional glycosphingolipidomics based on the selective enrichment of cellular GSLs onto aoGNP surface by applying the concept of glycoblotting. (b) Oxime bonds formed between GSL-aldehydes and aoGNPs are digested selectively by laser irradiation on MALDI process to afford highly sensitive iminoalcohol ions.

Figure 3. Profiling mouse brain glycosphingolipids by glycoblotting and subsequent MALDI-TOFMS. (a) GSLs identified in adult mouse brain (upper panel) and embryonic mouse (bottom panel). (b) MALDI-TOF/TOFMS analysis of the selected peak at *m/z* 1411.5 (GM1), 1702.6 (GD1a/GD1b), and 1993.6 (GT1b) observed in adult mouse brain. (c) MALDI-TOF/TOFMS of a precursor ion at *m/z* 1272.6 corresponding to GD3 detected in embryonic mouse brain.

Figure 4. Profiling whole GSLs enriched from mouse B16 melanoma cells (C57BL/6). (a) MALDI-TOFMS exhibited multiple ion peaks due to GSLs mixture observed in a range from *m/z* 1037.9 to 1140.1. (b) MALDI-TOF/TOFMS of a selected peak at *m/z*

1093.4 revealed that these GSLs are GM3 analogs having various *N*-acyl chains.

Figure 5. SPR analysis of GSL-GSL interaction on the basis of aoGNPs as a platform for displaying high-density GSLs (microdomains). GSLs-GNPs displaying whole GSLs from B16 mouse melanoma cells (-●-) or authentic (purified) GSLs such as GalCer (-◆-), LacCer (-■-), GM1 (-×-), and GM3 (-▲-) were employed as analytes for SPR-based binding assay with LB-membrane of Gg3Cer. Affinity constants (K_a) were calculated by using a common Langmuir-type equation: $[GSLs]/\Delta RU = [GSLs]/\Delta RU_{max} + 1/\Delta RU_{max}K_a$. Here, ΔRU_{max} means the maximal changes in the SPR upon the injection of the GSLs-GNPs. [GSLs] is the concentration of GSLs-GNPs and adjusted to be 0.01, 0.1, 0.5, 1.0, 2.5, 5.0, 7.5, and 10 μM.

cell

i) extraction

ii) ozonolysis

MS-based structural analysis

Cer

Cer

Cer

Cer

m/z

iii) GSLs-blotting

aoGNP

GSLs-GNP

SPR-based functional analysis

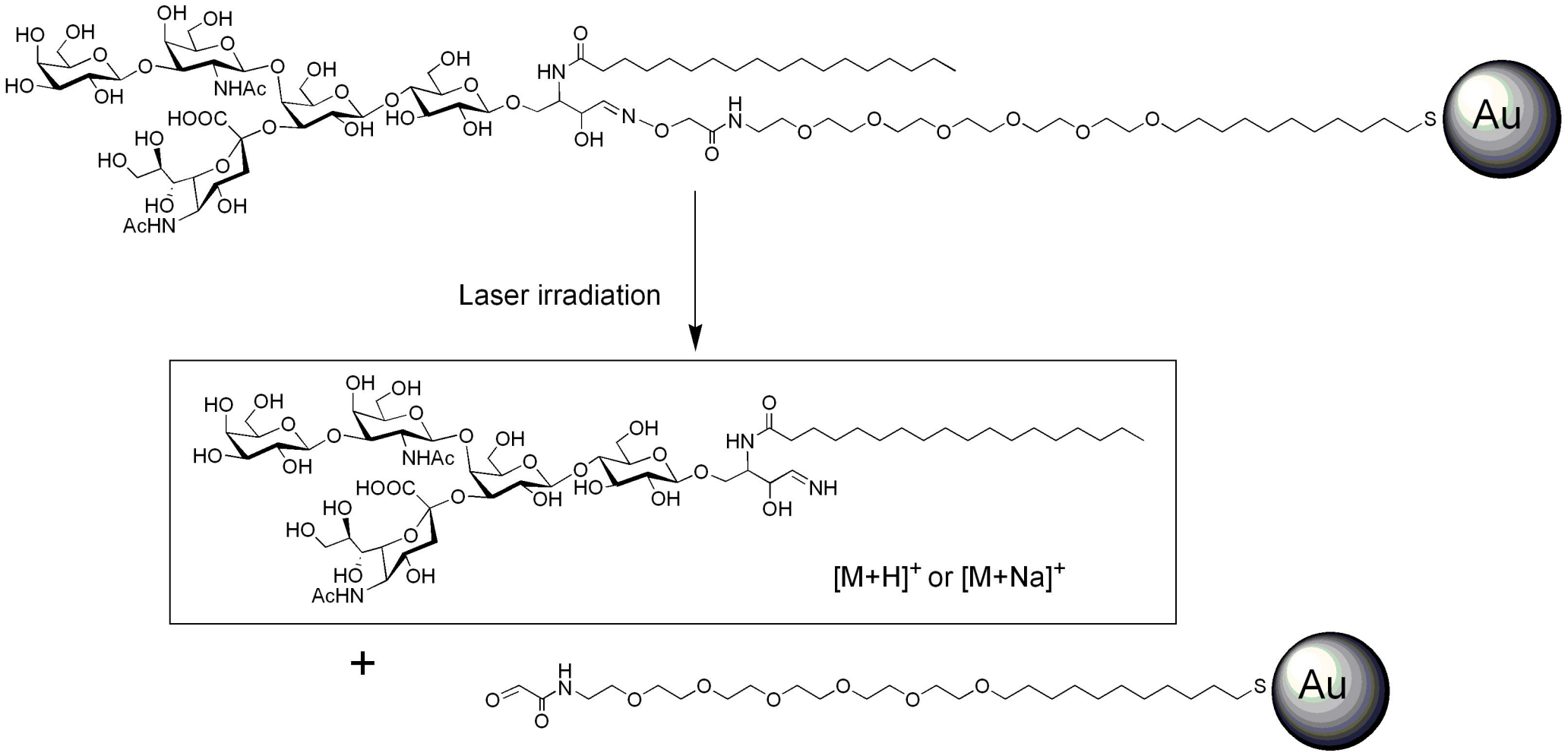
Au
Laser irradiation
[M+H]+ or [M+Na]+
+
Au

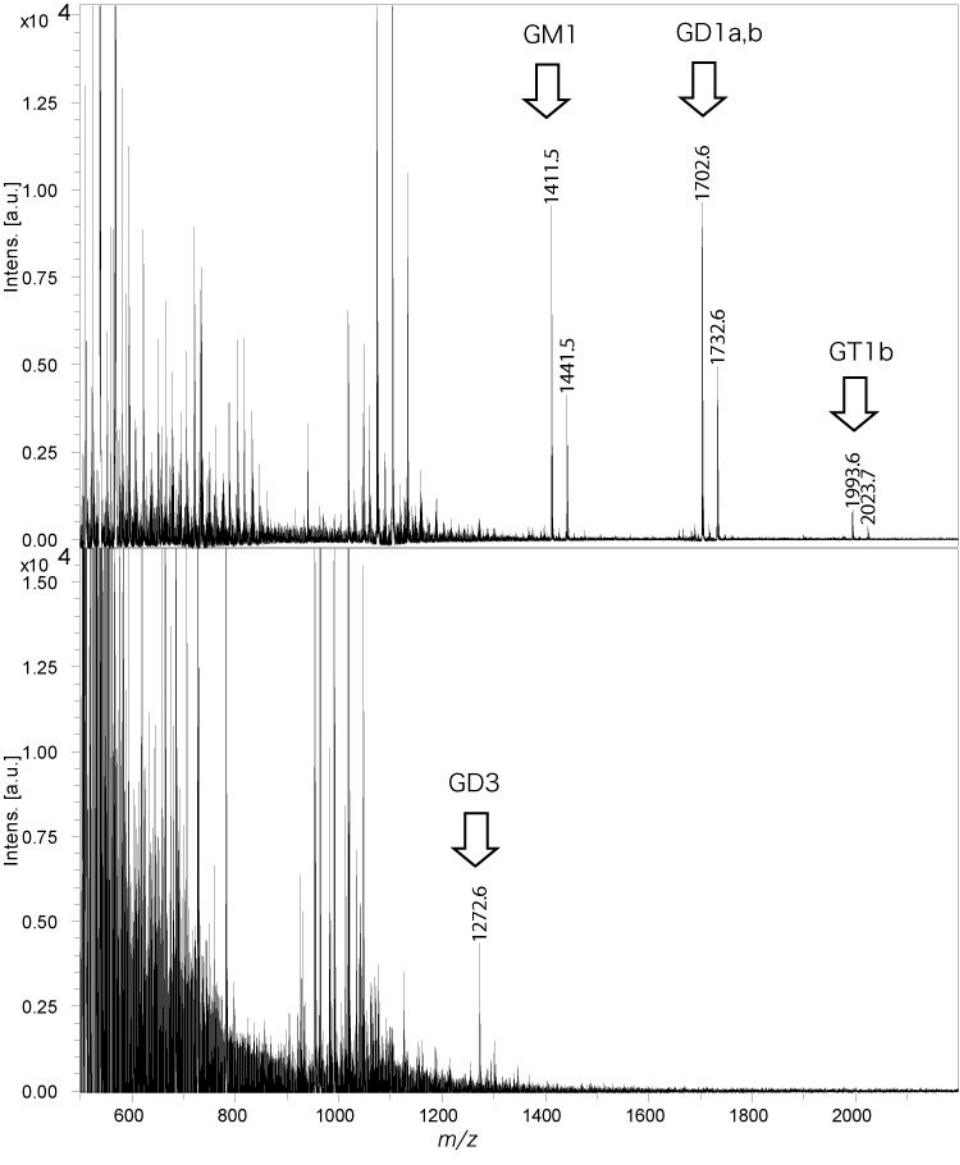
x10 4
1.25
1.00
0.75
0.50
0.25
0.00
Intens. [a.u.]
GM1
GD1a,b
1411.5
1702.6
1441.5
1732.6
GT1b
1993.6
2023.7
x10 4
1.50
1.25
1.00
0.75
0.50
0.25
0.00
Intens. [a.u.]
GD3
1272.6
600
800
1000
1200
1400
1600
1800
2000
m/z

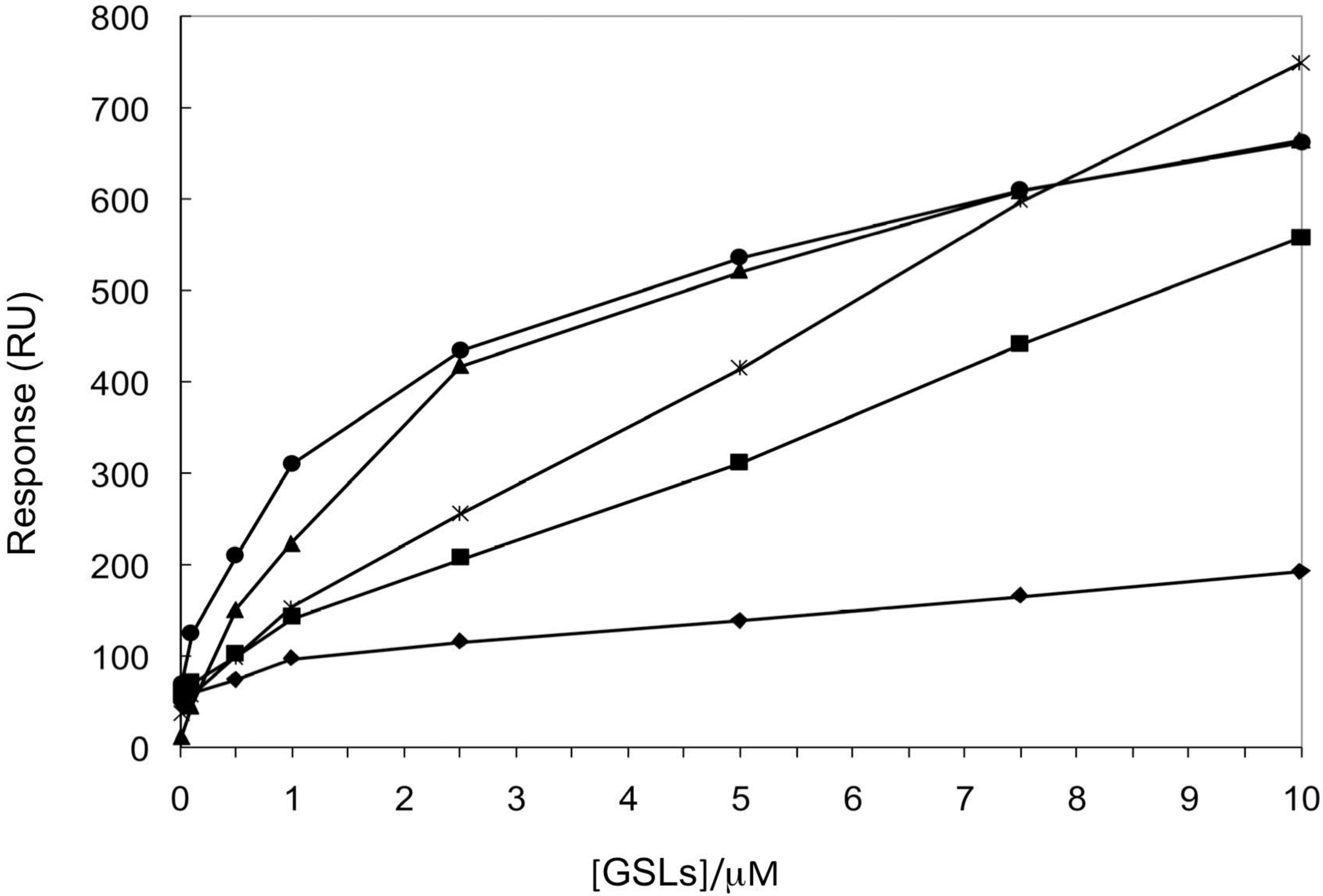
800
700
600
500
400
300
200
100
0
Response (RU)
0
1
2
3
4
5
6
7
8
9
10
[GSLs]/μM

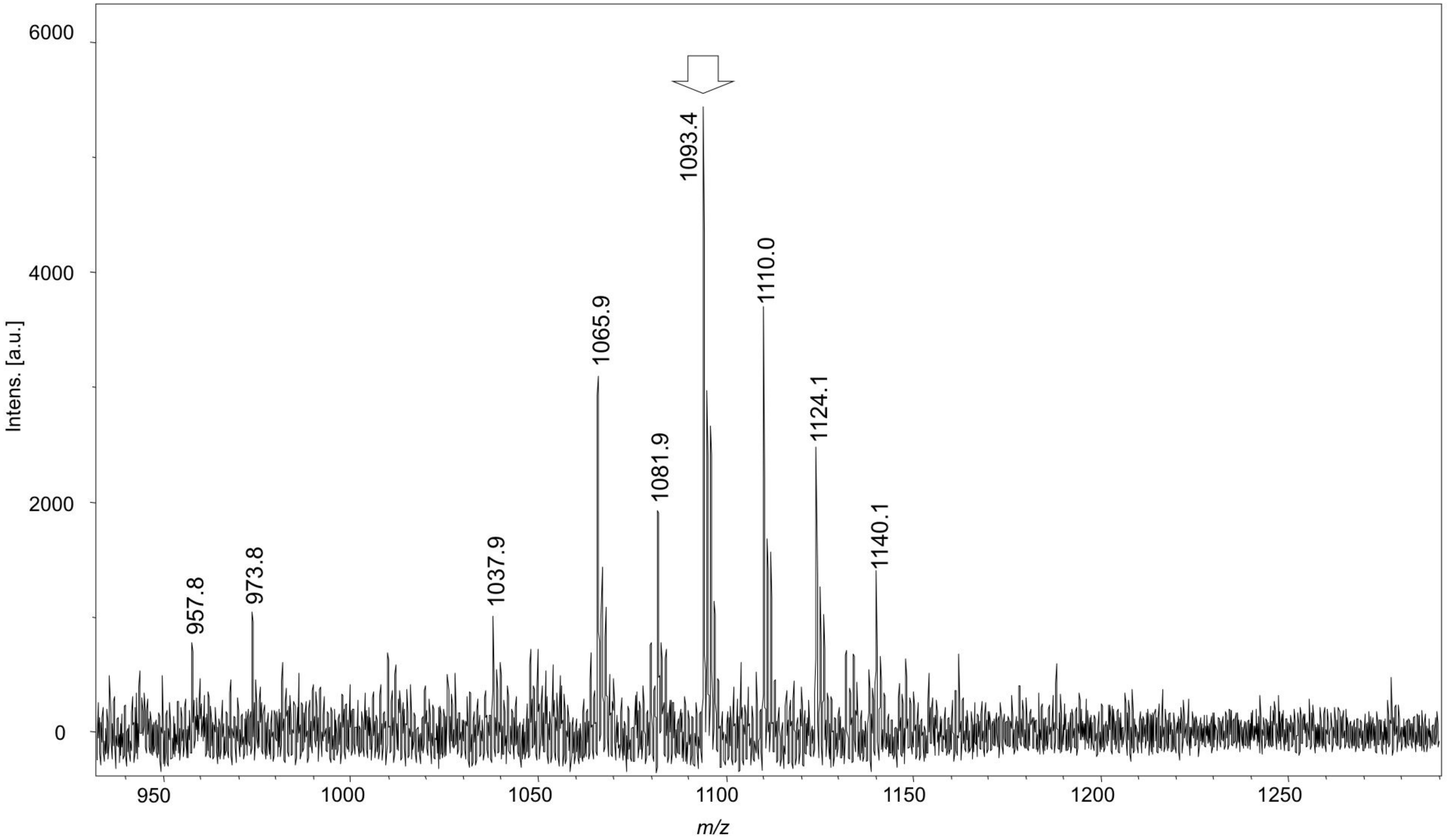
6000
4000
2000
0
Intens. [a.u.]
957.8
973.8
1037.9
1065.9
1081.9
1093.4
1110.0
1124.1
1140.1
950
1000
1050
1100
1150
1200
1250
m/z